IMPROVED DBO ALGORITHM FOR FIXED-WING UAV MOUNTAIN CROP IRRIGATION PATH PLANNING
/
改进的 DBO 算法用于固定翼无人机山地作物灌溉路径规划

Shengfu WU[1)], Peng ZHOU[1,2*)], Jin LUO[1)], Linjia CHUAN[1)], Jing LIU[1)], Fugui ZHANG[1,2*)]
[1)] School of Mechanical Engineering, Guizhou University, Guiyang, Guizhou/ China
[2)] Guizhou Provincial Key Laboratory of Mountainous Intelligent Agricultural Machinery, Guiyang, Guizhou/ China
Tel: 15286617318; E-mail: w15286617318@163.com
Corresponding author: Peng Zhou
Email address: pzhou@gzu.edu.cn, Guiyang, China
DOI: https://doi.org/10.35633/inmateh-79-42

Keywords: *Fixed-wing UAV; Path planning; Improved DBO algorithm; Safe turning radius; Pitch angle; Overlap ratio; Coverage uniformity*

ABSTRACT
To address the contradiction between obstacle avoidance safety and irrigation operation quality in 3D path planning of fixed-wing UAVs for mountainous agricultural crop irrigation, this paper proposes a multi-strategy improved dung beetle optimization (MDBO) algorithm. First, safe turning radius and pitch angle constraints are embedded into the optimization objective to restrict flight attitude, ensure flight stability under complex mountain terrain, reduce collision risk, and maintain consistent spray deposition. Second, four improvement strategies, including Bernoulli chaotic mapping initialization, golden sine position update mechanism, dynamic adaptive weight, and adaptive Gaussian-Cauchy hybrid mutation perturbation, are integrated into the basic DBO algorithm to enhance global search capability, local exploitation accuracy and convergence performance. Comparative tests on 9 benchmark functions show that MDBO outperforms the basic DBO in convergence speed and solution stability. Furthermore, three irrigation performance indicators (coverage rate, overlap ratio and coverage uniformity) are constructed for posterior evaluation of spray distribution quality. Simulation experiments under three mountainous terrain scenarios verify that MDBO achieves better path accuracy, convergence performance and irrigation effect than traditional algorithms, and can meet the efficient irrigation path requirements of mountainous agricultural crops.

摘要
为解决固定翼无人机在山区农业作物灌溉三维路径规划中避障安全性与灌溉作业质量之间的矛盾，本文提出一种多策略改进的蜣螂优化（MDBO）算法。首先，将安全转弯半径和俯仰角约束嵌入优化目标函数中，以限制飞行姿态，确保复杂山地地形下的飞行稳定性，降低碰撞风险，并保持喷洒沉积的一致性。其次，将伯努利混沌映射初始化、黄金正弦位置更新机制、动态自适应权重以及自适应高斯-柯西混合变异扰动等四种改进策略融入基本 DBO 算法，以提升全局搜索能力、局部开发精度和收敛性能。在 9 个基准函数上的对比实验表明，MDBO 在收敛速度和解的稳定性方面优于基本 DBO 算法。此外，构建了三个灌溉性能指标（覆盖率、重叠率和覆盖均匀性），用于对喷洒分布质量进行后评估。在三种山地地形场景下的仿真实验验证了 MDBO 算法在路径精度、收敛性能和灌溉效果方面优于传统算法，能够满足山地农作物高效灌溉路径的需求。

INTRODUCTION
In agricultural and forestry mountainous planting scenarios, irrigation is a key link in ensuring crop yield *(Ma, 2025)*. However, mountainous crop areas are restricted by objective conditions such as complex terrain (with interlaced slopes and gullies) *(Hu, 2023)* and uneven crop distribution (fruit tree clusters, terraced crops). Traditional ground irrigation equipment struggles to access these areas, and manual irrigation faces the dilemma of low efficiency and high cost.

Against this background, fixed-wing UAVs, with the advantages of long endurance and wide coverage, have become an ideal carrier for irrigation in agricultural and forestry mountainous areas—by carrying spray or drip irrigation components, they can achieve large-area and efficient irrigation operations.

As one of the core issues in fixed-wing UAV irrigation operations, the quality of irrigation path planning *(Giagkiozis et al., 2015)* directly determines the irrigation effect: it is necessary to ensure that the path fully covers all areas to be irrigated, while avoiding obstacles such as fruit tree canopies and slope shoulders, and to maintain a stable flight process to prevent uneven irrigation caused by severe attitude changes. In agricultural aviation, flight stability and path smoothness are critical not only for geometry but also for spray deposition uniformity, droplet drift mitigation, and operational continuity. Studies on UAV-based spraying have shown that flight parameters such as altitude, velocity, and operational stability significantly influence droplet coverage, deposit consistency, and drift risk *(Wang et al., 2017; Wang et al., 2017; Pan et al., 2016)*. Furthermore, the spray distribution from a UAV is inherently non-uniform, and the coverage uniformity is critically affected by flight speed and pass width *(Nanavati et al., 2023)*. Therefore, optimizing path planning for irrigation requires not only obstacle avoidance and path length minimization but also consideration of spray coverage uniformity and overlap control.

In terms of flight parameter constraints *(Deng et al., 2022)*, in traditional path planning, UAVs are often simplified as point masses. However, fixed-wing UAVs have a large volume and may collide with obstacles during flight; moreover, they require long takeoff and landing distances. In addition, UAVs need to frequently adjust their flight trajectories between crops and slopes in agricultural and forestry mountainous areas. If parameter constraints are not fully considered in traditional planning, a series of problems are likely to occur: if the turning radius is too small, UAVs are prone to colliding with fruit trees or slope ridges; if the pitch angle fluctuates too much, it will lead to unstable flight altitude (excessively high altitude causes uneven diffusion of irrigation liquid/droplets, while excessively low altitude may scratch crops). Therefore, it is crucial to introduce constraints on the two flight parameters of safe turning radius and pitch angle in irrigation path planning for agricultural and forestry mountainous areas—which is also the key that distinguishes this scenario from ordinary mountain path planning, as the irrigation scenario has more prominent requirements for "path coverage integrity" and "flight attitude stability."

In terms of path planning algorithms, traditional path planning algorithms such as Dijkstra's algorithm *(Fadzli et al., 2015)*, artificial potential field (APF) method *(Zhou et al., 2015)*, and simulated annealing (SA) algorithm *(Zhu et al., 2006)* have the problem of slow convergence, making it difficult to adapt to the dynamically changing needs of crop distribution in agricultural and forestry mountainous areas. Although existing intelligent optimization algorithms such as the A* algorithm *(Wang et al., 2023)*, genetic algorithm (GA) *(Zhao et al., 2023)*, ant colony optimization (ACO) algorithm *(Wen et al., 2023)*, and particle swarm optimization (PSO) algorithm *(Chen et al., 2023)* have been applied in related fields, they still have the defect of being prone to falling into local optimality (e.g., only avoiding local fruit tree clusters while ignoring marginal irrigation areas). *Zhu et al., 2006,* proposed a path planning method for plant protection UAVs based on the genetic algorithm: by converting intra-regional operation paths and inter-regional scheduling paths into virtual nodes or arcs to construct a super network, it verified the feasibility of this method in the multi-plot path planning problem of UAV pesticide spraying. *Wang et al., (2023),* improved the ant colony algorithm by introducing a height factor, making the ant colony search more directional. *Zhao et al., (2023),* proposed an improved particle swarm UAV trajectory planning algorithm: by combining the "stepwise" adjustment strategy of inertia weight and the strategy of jumping out of local optimal solutions, it improved the optimality and real-time performance of the planning algorithm.

In the context of agricultural spraying operations, coverage path planning has been extensively studied. *Vazquez-Carmona et al., (2022),* proposed a CPP method for spraying drones that models the sprinkler footprint as a paraboloid and restricts flight within the region of interest to avoid collisions. *Plessen, (2025),* combined the traveling salesman problem with area coverage path planning for spot spraying, demonstrating that the inclusion of headland paths significantly reduces coverage gaps. *Meron et al., (2025),* employed high-resolution thermal and visible light imagery to quantify irrigation uniformity across surface, linear move, and solid-set irrigation systems, using the Crop Water Stress Index and Christiansen Uniformity Coefficient as evaluation metrics. *Cui et al., (2025),* utilized UAV multispectral imagery to estimate soil salinity under sunflower cover, demonstrating the feasibility of UAV-based monitoring for precision irrigation management.

Although the above algorithms can improve path planning performance to some extent, their application to mountainous crop irrigation remains limited when coverage continuity and terrain-adaptive flight stability must be considered simultaneously. For irrigation or spraying UAVs, trajectory optimization is not only a geometric problem; it also affects the continuity of the effective spray swath, local overlap/gap formation, and the stability of relative altitude above the crop canopy.

Existing studies on spraying path planning have shown that coverage-gap avoidance and area-coverage organization are essential for practical aerial application, rather than only minimizing route length. In addition, studies on UAV aerial spraying have reported that flight parameters such as height, velocity, and operational stability directly influence droplet coverage, deposit consistency, and drift risk.

Therefore, in the irrigation of mountain crops, a feasible approach should simultaneously meet the requirements of obstacle avoidance, fixed-wing kinematic constraints, and flight stability for irrigation. To address these challenges, the basic DBO framework was retained and enhanced by Bernoulli chaotic initialization, a golden sine strategy, dynamic adaptive weights, and an adaptive Gaussian-Cauchy mixed perturbation strategy, thereby proposing a multi-strategy DBO (MDBO). The optimization objective of this algorithm is to search for the shortest feasible path that satisfies the flight constraints such as smooth turning, stable pitch, and terrain adaptability, while ensuring the safety constraints. On this basis, this study introduces three irrigation performance indicators - coverage, repetition, and coverage uniformity - after the path planning is completed for posterior evaluation of the spray distribution quality of the optimized path. This design effectively overcomes the problems of local optimization and poor stability of fixed-wing unmanned aircraft in path planning in this scenario, and provides a quantitative evaluation basis for the applicability of the planned path for irrigation.

MATERIALS AND METHODS

Fixed-Wing UAV Path Planning Modelling

Mountain Modelling

To simulate the real mountainous irrigation environment, a 3D terrain model is constructed by superposition of multiple Gaussian hills, which can accurately reflect the elevation fluctuation characteristics of mountainous areas, as shown in Fig. 1.

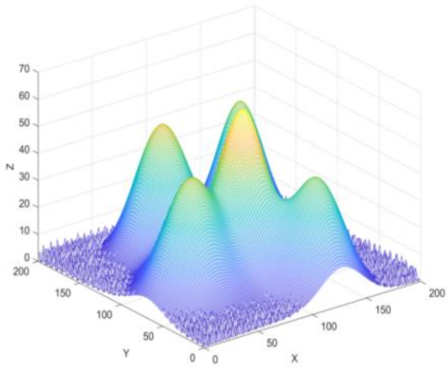

Fig. 1 - Mountain model

The mathematical expression is:

$$Z(x,y)=\sum_{i=1}^{N}h_i\exp[\left(\frac{x-x_{ic}}{x_{ir}}\right)^2-\left(\frac{y-y_{ic}}{y_{ir}}\right)^2 \tag{1}$$

where: N is the number of hills; h_i is the height; (x_{ic},y_{ic}) is the center coordinate; x_{ir} is the gradient along the x-axis; and y_{ir} is the gradient along the y-axis.

Objective Function

Suppose that a fixed-wing UAV passes through N nodes during operation, with coordinate (x_1,y_1,z_1), (x_2,y_2,z_2), …, (x_N,y_N,z_N). The objective function consists of four core terms:

(1) The total length of the fixed-wing UAV path:

$$F_1=\sum_{i=1}^{N-1}\sqrt{dx_i^2+dy_i^2+dz_i^2} \tag{2}$$

where: F_1 represents the total length of the entire path, dx_i is the distance between two path nodes in the X-axis direction, dy_i is the distance between two path nodes in the Y-axis direction, dz_i is the distance between two path nodes in the Z-axis direction, and N represents the total number of path nodes.

(2) Path altitude of fixed-wing UAV:

$$F_2 = \sum_{i=1}^{N} \left| Z_i - \bar{Z} \right| \tag{3}$$

where: F_2 represents the path height, Z_i represents the z-coordinate of the i-th path point, $\bar{Z}$ represents the mean of all z-coordinates, and N represents the total number of path nodes.

(3) Safe turning radius for fixed-wing UAV:

$$F_3 = \sum_{i=1}^{N-2} \left(\cos\frac{\pi}{2} - \frac{dx_i \cdot dx_{i+1} + dy_i \cdot dy_{i+1} + dz_i \cdot dz_{i+1}}{\sqrt{dx_i^2 + dy_i^2 + dz_i^2} \cdot \sqrt{dx_{i+1}^2 + dy_{i+1}^2 + dz_{i+1}^2}} \right) \tag{4}$$

where: F_3 represents the safe turning radius, dx_i represents the variation of the i-th path segment on the x-coordinate, dy_i represents the variation of the i-th path segment on the y-coordinate, dz_i represents the variation of the i-th path segment on the z-coordinate, and dx_{i+1} represents the variation of the i+1st path segment on the x-coordinate, dy_{i+1} represents the variation of the i+1st path segment on the Y-coordinate, dz_{i+1} represents the variation of the i+1st path segment on the Z-coordinate, and N_2 represents the total number of path nodes.

(4) Pitch Angle of fixed-wing UAV flight:

$$F_4 = \tan^{-1}\left(\frac{dz}{\sqrt{dx^2 + dy^2}} \right) \tag{5}$$

where: F_4 represents the pitch Angle.

(5) Overall objective function expression:

$$F = \sum_{i=1}^{4} w_i \times F_i \tag{6}$$

where: $w_1 \sim w_4$ are weight coefficients, balancing path efficiency, flight safety and irrigation performance. The optimal weight combination is determined by ablation experiments.

Irrigation Performance Indicators

Different from ordinary path planning, irrigation path planning needs to evaluate the actual operation effect. Three quantitative indicators are proposed for posterior evaluation of spray distribution quality, which are not involved in the optimization process.

(1) Coverage rate: The proportion of grids sprayed at least once in the target area, reflecting the integrity of irrigation coverage.

$$CR = \frac{|\{(i,j) \mid c_{i,j} \geq 1\}|}{N_x \times N_y} \tag{7}$$

where: $c_{i,j}$ represents the coverage times of the grid (i,j), N_x and N_y represent the total number of grids in each dimension.

(2) Overlap ratio: The proportion of grids with spray times exceeding the ideal threshold, reflecting the degree of resource waste caused by repeated spraying.

$$OR = \frac{|\{(i,j) \mid c_{i,j} > c_{\text{ideal}}\}|}{N_x \times N_y} \tag{8}$$

where: c_{ideal} represents the ideal coverage threshold.

(3) Coverage uniformity: Quantifying the uniformity of spray distribution in the covered area. The closer the value is to 1, the more uniform the spray distribution.

$$U = 1 - \frac{\sigma(c_{\text{covered}})}{\mu(c_{\text{covered}})} \tag{9}$$

where: μ and σ represent the mean and standard deviation of the total number of times all covered grids have been covered, respectively.

Dung Beetle Optimization Algorithm

Dung Beetle Optimization Algorithm (DBO) is a novel population-based intelligence optimization algorithm inspired by social behaviors of dung beetles during the acquisition and handling of dung balls *(Xue et al., 2023)*.

As an innovative algorithm, dung beetles search rolling burying and guarding dung balls to implement the meta-heuristic as a means of dealing with complex optimization problems. More specifically, the DBO simulates 5 main behaviors of dung beetles — rolling of the ball, dance, mating, foraging and pill stealing *(Jin et al., 2023)*.

Rolling beetles move forward along a straight trajectory with the aid of light sources; dancing behavior adjusts moving direction when encountering obstacles; breeding beetles update positions within local optimal areas for oviposition; foraging beetles search for food near the global optimum with normal distribution perturbation; thief beetles compete for dung balls near the optimal food source to increase population diversity.

The basic DBO algorithm has fast initial convergence, but it still has limitations in solving complex 3D path planning problems: random initialization leads to insufficient population diversity, and population aggregation in the late iteration stage easily causes premature convergence and falls into local optimum. To address these defects, this paper improves the algorithm from four aspects to enhance its adaptability to mountainous irrigation path planning scenarios.

An Advanced Multiple Strategies Dung Beetle Optimization Algorithm

Aiming at the defects of basic DBO algorithm, four improvement strategies are integrated to construct a multi-strategy improved dung beetle optimization (MDBO) algorithm, so as to balance global exploration and local exploitation capability and avoid premature convergence.

Bernoulli Chaotic Mapping Strategy

Random initialization easily leads to uneven population distribution and insufficient diversity, limiting the early global search range. Chaotic mapping features ergodicity, randomness and regularity, which can generate initial populations with wider distribution and better diversity. In this paper, Bernoulli chaotic mapping is used to generate initial population positions *(Saito et al., 2016)*. The mapping expression is:

$$z_{n+1}=\begin{cases}\dfrac{z_n}{1-\beta}, & 0\le z_n\le 1-\beta\\[2ex] \dfrac{z_n-(1-\beta)}{\beta}, & 1-\beta\le z_n\le 1\end{cases} \tag{10}$$

where: $\beta\in(0,1)$.

Golden Sine Strategy

In the basic DBO algorithm, the position update of rolling beetles lacks sufficient information interaction with the optimal individual, which is easy to cause premature convergence. The golden sine algorithm combines the golden section ratio with the sine position update mechanism, which can effectively balance global exploration and local exploitation.

This paper introduces the golden sine strategy to optimize the position update of rolling beetles. The update formula is:

$$X_i^{t+1}=X_i^t\times|\sin(R_1)|+R_2\times\sin(R_1)\times|x_1\times P_i^t-x_2\times X_i^t| \tag{11}$$

where: $R_1\in(0,2\pi)$, $R_2\in(0,2\pi)$, $x_1=-\pi+(1-\tau)*2\pi$, $x_2=-\pi+(1-\tau)*2\pi$, $\tau(\tau=(\sqrt{5}-1)/2)$.

In the second part of the position update expression, if $R_2<ST$, the dung beetle gradually reduces its angle; otherwise $R_2\geqslant ST$, the dung beetle has a random walk in normal distribution in the same region. While this design allows the algorithm to converge to the global best solution at the start of the fitness iteration, it also increases the potential to converge too quickly and get stuck at local optima. In order to remedy this defect, the present work proposed the golden sine, to optimize the DBO algorithm partition update mechanism. Below is the updated version of position update Equation:

$$X_{i,j}^{t+1}=\begin{cases}X_{ij}^t\times|sin(R_1)|+R_2\times sin(R_1)\times|x_1\times X_{best}^t-x_2\times X_{ij}^t|, R_2<ST\\[2ex] X_{i,j}^t+Q\cdot L, \quad R_2\ge ST\end{cases} \tag{12}$$

The improved position update scheme enhances algorithm performance in two aspects. First, all individuals interact with the current optimal individual per iteration to fully exploit optimal information, which remedies the deficiency of inter-individual information exchange in the original DBO. Second, the golden sine strategy broadens the search range to avoid local optima, and the golden section coefficient fine-tunes the search distance and direction of dung beetles, thus achieving a balanced trade-off between global exploration and local exploitation.

Strategy For Dynamic Adaptability Weight

While, given many early iterations of the DBO algorithm, the algorithm may over-focus onto local areas, causing local convergence. To overcome this drawback, in this paper, the position update formula is changed by adding between its own position the global optimal solution from last generation, which means during the current position update, the position will be affected not only by itself but its optimal solution in the previous generation. Moreover, dynamic weight coefficient is proposed to improve global search ability in the early stage, whilst increasing local search and convergence processes in the latter stages by reducing adaptation. The new coefficient w and the new position update equations are as follows:

$$w = \frac{e^{2(1-t/iter_{max})} - e^{-2(1-t/iter_{max})}}{e^{2(1-t/iter_{max})} + e^{-2(1-t/iter_{max})}} \tag{13}$$

$$X_{i,j}^{t+1} = \begin{cases} (X_{i,j}^{t} + w(f_{j,g}^{t} - X_{i,j}^{t})) \cdot rand, R_2 < ST \\ X_{i,j}^{t} + Q, \qquad\qquad R_2 \geq ST \end{cases} \tag{14}$$

where: $f_{j,g}^{t}$ is the j-th dimensional global optimal solution of the previous generation; Q is the stochastic number; $R_2 \in (0,1)$; and $ST \in (0.5,1)$.

Adaptive Gauss-Cauchy Mixed-Variance Perturbation Strategy

In later iterations, the basic DBO suffers from severe population aggregation around local optima. While accelerating convergence, this phenomenon sharply reduces population diversity, trapping the algorithm in local minima and even causing search stagnation. Mutation perturbation is a widely adopted technique to restore population diversity and assist the algorithm in escaping local optima *(Du et al., 2024)*.

Among common mutation operators, Gaussian mutation achieves fine local exploitation with small step sizes, whereas Cauchy mutation performs broader global exploration with larger step sizes but may generate lower-quality offspring. To fully leverage the strengths of both, this paper proposes an adaptive Gaussian-Cauchy hybrid mutation perturbation strategy. It only applies perturbation to the current best individual, and retains the mutated position only when its fitness is improved, thus effectively expanding population diversity while guaranteeing solution quality. The specific expression is given as follows:

$$H^b(t) = X^b(t) * (1 + \mu_1 * Gauss(\sigma) + \mu_2 * cauchy(\sigma)) \tag{15}$$

where: $\mu_1 = t / T_{max}$, $\mu_2 = 1 - t / T_{max}$, $X^b(t)$ indicates the individual's optimal position at the t-th iteration, $H^b(t)$ represents the position of the optimal position post a mixed Gauss-Cauchy perturbation, $Gauss(\sigma)$ is the Gaussian variational operator, and $cauchy(\sigma)$ is the Cauchy variational operator.

The strategy applies adaptive perturbation throughout iterations, with mutation modes dynamically tuned to the population distribution state. In early iterations, Cauchy distribution with large-amplitude perturbations is adopted for the widely dispersed population, which enhances population diversity, boosts global search capability, and prevents premature trapping in local optima. As iterations proceed and the population gradually converges, Gaussian distribution with small-amplitude perturbations dominates to perform precise local exploitation, accelerating convergence while maintaining algorithmic robustness in complex high-dimensional spaces. This adaptive switching mechanism effectively achieves a balanced trade-off between global exploration and local exploitation.

The mechanics and flow of this approach are encapsulated in the pseudo-code for the MDBO algorithm, which is detailed in Table 1 below.

Table 1

Pseudo-code for the MDBO algorithm

Pseudo-code for the MDBO algorithm
Inputs: maximum number of iterations T_{max} , population size N .
Output: optimal position X^b and its fitness value f_b .
Randomly initialize the dung beetle population, defining the relevant parameters
Initialization of population positions using Bernoulli's chaotic mapping
while $(t \le T_{max})$ **do**
for $i \leftarrow 1\ to\ N$ **do**
if $i ==$ Dung Beetle Roller **then**
$\delta = \text{rand}(1)$
if $\delta < 0.9$ **then**
Use the golden sine strategy to update the position of the rolling dung beetle;
else
Update the position of the rolling dung beetle;
end if
end if
if i ==Breeding Dung Beetles **then**
Update the location of breeding dung beetles;
end if
if i ==Foraging Dung Beetle **then**
The location of the foraging dung beetle was updated;
end if
if i ==Stealing Dung Beetles **then**
Updating the location of the stealing dung beetle using a equation that incorporates dynamic weighting factors;
end if
end for
If the newly generated position is better than before
Update Location;
end if
Applying an adaptive Gauss-Cauchy mixed-variance perturbation strategy to the current optimal solution
if the position is better after perturbation
Accept new position;
end if
$t = t + 1$
end while
Return the fitness value

Application of the MDBO Algorithm to Fixed-Wing UAV Path Planning

The procedure for applying the MDBO algorithm to fixed-wing UAV path planning is as follows:

Step1: Define start and end points, and construct a detailed map of complex mountain terrain;

Step2: Enter the objective function and associated parameters to guide the search;

Step3: Position the dung beetles using Bernoulli's chaotic mapping to ensure diverse starting points;

Step4: Calculate the fitness of each individual based on the objective function within the designated fitness landscape;

Step5: Apply the golden sine algorithm to adjust the positions of all dung beetles towards optimal paths;

Step6: Verify that no dung beetle exceeds the predefined map boundaries;

Step7: Modify current positions by integrating influences from both the previous positions and the current best solution using a dynamic adaptive weighting strategy;

Step8: Refresh the best-known solution and its corresponding fitness score;

Step9: Employ an adaptive Gauss-Cauchy mixed-variance perturbation strategy to further refine the current best solution, creating potential new optimal paths;

Step10: Determine if the end condition is met; if not, loop back to Step 4; if yes, proceed to the final step;

Step11: Deliver the optimal path solution with its fitness value and conclude the algorithm.

Refer to the flowchart depicted in Fig. 2 for a graphical representation of the MDBO algorithm steps.

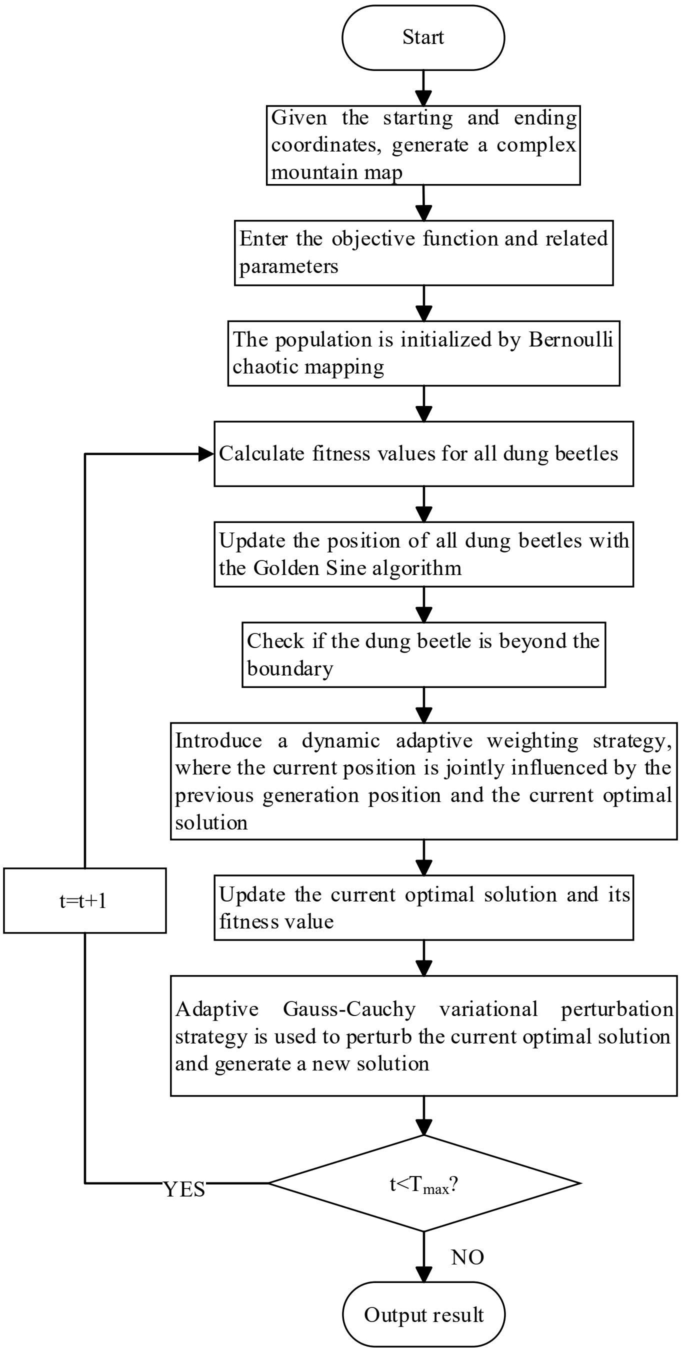

Fig. 2 - The flowchart of the MDBO algorithm

RESULTS

The experiments were conducted on a computer equipped with an Intel® Core™ i5-8250U processor operating at 1.60–1.80 GHz and 16 GB of RAM. The system ran the 64-bit version of Windows 11, and MATLAB R2022b was used for all simulations.

Security Constraints Impact Analysis

Safe turning radius and pitch angle are critical constraints for fixed-wing UAV path planning. Neglecting these constraints will induce excessively sharp turns and abrupt pitch maneuvers, which degrade flight efficiency, elevate collision risks and reduce spray uniformity in complex terrain. Comparative experiments with and without the above constraints are carried out, with results shown in Fig. 3. It is verified that introducing the constraints yields a smoother flight path with gentler turning and climbing maneuvers, thus effectively improving flight safety and operational reliability.

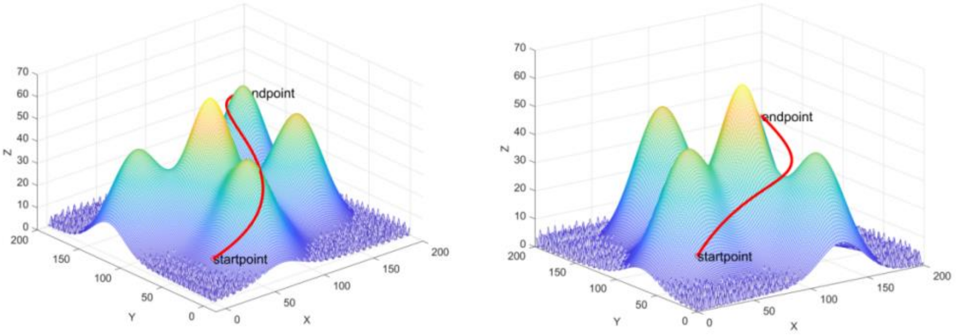

a) b)

Fig. 3 - Comparison of experiments with and without constraints

(a) No safe turning radius and pitch angle constraints; (b) Add safe turning radius and pitch angle constraints

Performance Analysis of the Algorithm Using Benchmark Test Functions

To gauge the effectiveness of the modified MDBO algorithm, this research utilized nine benchmark test functions outlined in Table 2. These functions were used to test and compare the MDBO algorithm against the original DBO algorithm. The chosen benchmarks encompass single-peak, multi-peak, and fixed-dimension functions, providing a comprehensive evaluation across various optimization scenarios. For each algorithm, the testing conditions were standardized with a population size of 30 and a limit of 500 iterations.

Each algorithm was independently run 30 times on the nine benchmark test functions, and the optimal value, mean, and standard deviation of the function values were recorded. The computational results are displayed in Table 3. As shown in Table 3, the results of the comprehensive experiments across the nine test functions indicate that the MDBO algorithm achieves optimal values comparable to the DBO algorithm on the 7th and 8th functions. Additionally, for the 9th function, both algorithms yield identical results. For the remaining six functions, the MDBO algorithm demonstrates superior optimization accuracy compared to the DBO algorithm. Furthermore, in terms of computational stability, the MDBO algorithm exhibits a lower standard deviation over 30 runs, indicating higher consistency and enhanced search capability compared to the DBO algorithm.

Table 2

Benchmark test function

Benchmark test function	Dimension	Definition	f_{min}
$F_1(x)=\sum_{i=1}^{n}x_i^2$	30	[-100,100]	0
$F_2(x)=\sum_{i=1}^{n}\lvert x_i\rvert+\prod_{i=1}^{n}\lvert x_i\rvert$	30	[-10,10]	0
$F_3(x)=\sum_{i=1}^{n}\left(\sum_{j-1}^{i}x_i\right)^2$	30	[-100,100]	0
$F_4(x)=\sum_{i=1}^{n}ix_i^4+random[0,1)$	30	[-128,128]	0
$F_5(x)=\sum_{i=1}^{n}\left[x_i^2-10\cos(2\pi x_i)+10\right]$	30	[-5.12,5.12]	0
$F_6(x)=-20\exp\left(-0.2\sqrt{\frac{1}{n}\sum_{i=1}^{n}x_i^2}\right)-exp\left(\frac{1}{n}\sum_{i=1}^{n}\cos(2\pi x_i)\right)+20+e$	30	[-32,32]	0
$F_7(x)=\frac{1}{4000}\sum_{i=1}^{n}x_i^2-\prod_{i=1}^{n}cos\left(\frac{x_i}{\sqrt{i}}\right)+1$	30	[-600,600]	0
$F_8(x)=\sum_{i=1}^{11}\left[a_i-\frac{x_1\left(b_i^2+b_ix_2\right)}{b_i^2+b_ix_3+x_4}\right]^2$	4	[-5,5]	0.0003075
$F_9(x)=\left(x_2-\frac{5.1}{4\pi^2}x_1^2+\frac{5}{\pi}x_1-6\right)^2+10\left(1-\frac{1}{8\pi}\right)cosx_1+10$	2	[-5,5]	0.398

Table 3

Benchmark test function experimental results

Function	Evaluation indicators	DBO	MDBO
	optimal value	4.7424E-158	0.00E+00
F1	mean	2.5287E-114	0.00E+00
	standard deviation	1.3785E-113	0.00E+00
	optimal value	1.2751E-167	0.00E+00
F2	mean	3.737E-109	0.00E+00
	standard deviation	2.0468E-108	0.00E+00
	optimal value	1.3035E-79	0.00E+00
F3	mean	4.0589E-59	3.4453E-293
	standard deviation	1.9479E-58	0.00E+00
	optimal value	8.6575E-4	24572E-4
F4	mean	0.5819	0.0328
	standard deviation	0.3549	0.0549
	optimal value	2.3283E-4	1.7876E-06
F5	mean	1.4341E-3	1.2686E-4
	standard deviation	9.4036E-4	1.2383E-4
	optimal value	2.7046E-188	0.00E+00
F6	mean	3.5662E-115	0.00E+00
	standard deviation	1.8311E-114	0.00E+00
	optimal value	0.00E+00	0.00E+00
F7	mean	0.1005	0.00E+00
	standard deviation	0.5503	0.00E+00
	optimal value	3.0749E-4	3.0749E-4
F8	mean	6.4466E-4	3.1581E-4
	standard deviation	3.5861E-4	2.6591E-05
	optimal value	0.3979	0.3979
F9	mean	0.3979	0.3979
	standard deviation	0.00E+00	0.00E+00

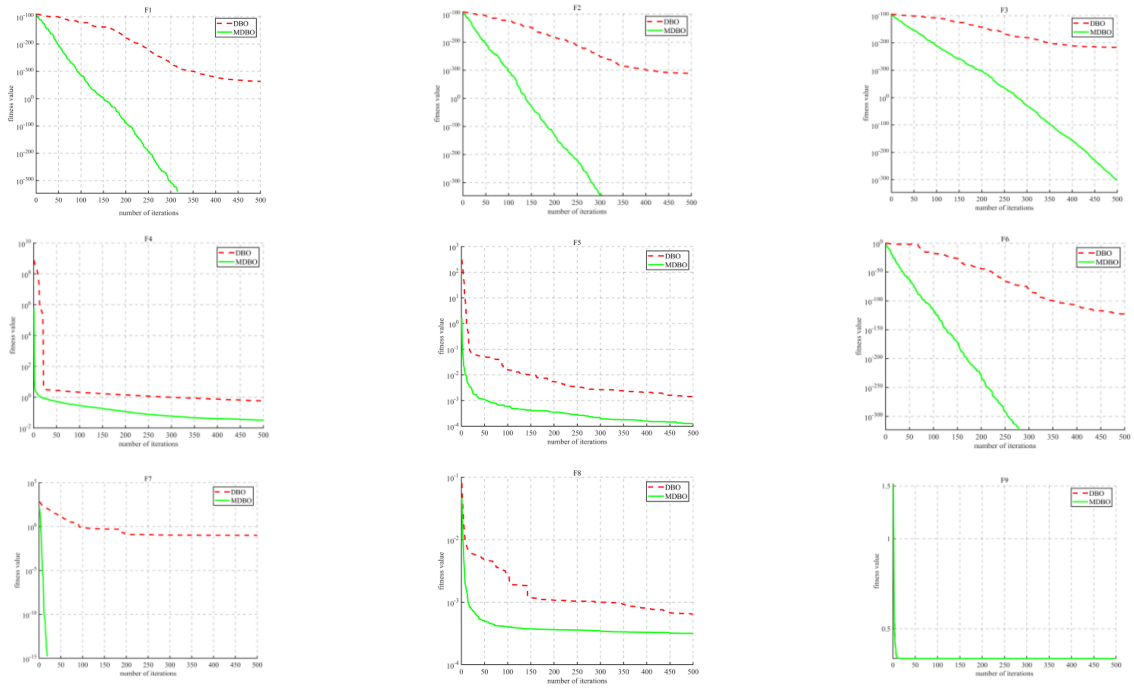

Fig. 4 - Convergence curves for each algorithm

Performance Analysis of the Algorithm Using Benchmark Test Functions

As the weight parameters of the multi-objective function directly determine path planning performance, this section adopts the single-factor control variable method in ablation experiments to analyze the influence law of each weight on fixed-wing UAV mountain irrigation path planning, and determines the optimal weight combination applicable to mountain agricultural irrigation scenarios.

The objective function consists of four core terms: path length, altitude fluctuation, turning radius constraint and pitch angle constraint, corresponding to weights w_1, w_2, w_3 and w_4 respectively. During the experiment, three weights are fixed at the final determined values, and only the target weight is adjusted within the range of [0, 1] with a step size of 0.1. Each parameter set undergoes 30 independent repeated experiments, and the error bars in the figures represent the standard deviation of results to quantify the operational stability of the algorithm.

Figs. 5–8 present the influence of each weight coefficient on path planning performance obtained via single-factor ablation experiments.

For the path length weight w_1 (Fig. 5): increasing w_1 within 0–0.3 significantly reduces altitude fluctuation, turning cost and pitch angle cost without notable path length degradation. At w_1 = 0.3, altitude fluctuation and pitch angle cost reach the global minimum, and turning cost stays within the optimal range. Values above 0.3 cause sharp deterioration of attitude-related indicators despite marginal reduction in path length, so w_1 = 0.3 is selected.

For the altitude fluctuation weight w_2 (Fig. 6): as w_2 rises from 0 to 0.3, altitude fluctuation drops sharply from 1200 m to 220 m, accompanied by optimized turning and pitch angle costs. When w_2 exceeds 0.3, altitude fluctuation oscillates without further improvement, while path length and attitude-related costs all deteriorate. Thus w_2 = 0.3 is adopted.

For the turning radius weight w_3 (Fig. 7): as a hard safety constraint for fixed-wing UAVs, insufficient turning radius directly leads to aerodynamic stall and crash. Increasing w_3 below 0.65 gradually optimizes turning cost without obvious degradation of other indicators, while values above 0.65 cause significant deterioration of path length, altitude fluctuation and pitch angle cost. Prioritizing flight safety, w_3 = 0.65 is determined.

For the pitch angle weight w_4 (Fig. 8): pitch angle cost keeps optimizing with the growth of w_4. Within the range of w_4 in [0.3, 1], pitch angle cost stabilizes in the optimal interval of 0.09–0.11, and no significant degradation occurs in path length, altitude fluctuation or turning cost. Given that pitch angle constraint directly determines operational feasibility, w_4 = 1.0 is chosen.

Based on the above experimental results, the final multi-objective weight combination applicable to mountain agricultural irrigation scenarios is determined as w_1 = 0.3, w_2 = 0.3, w_3 = 0.65, w_4 = 1.0.

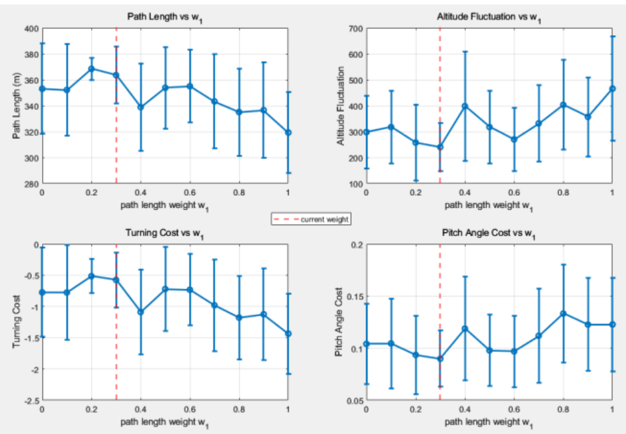

Fig. 5 - The influence of path length weight w_1 on the performance of path planning

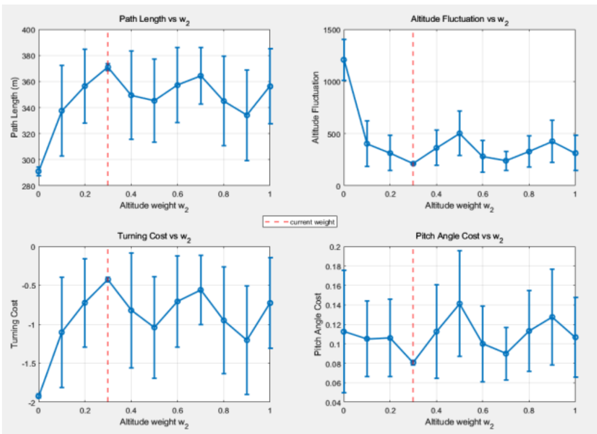

Fig. 6 - The influence of the highly fluctuating weight w_2 on the performance of path planning

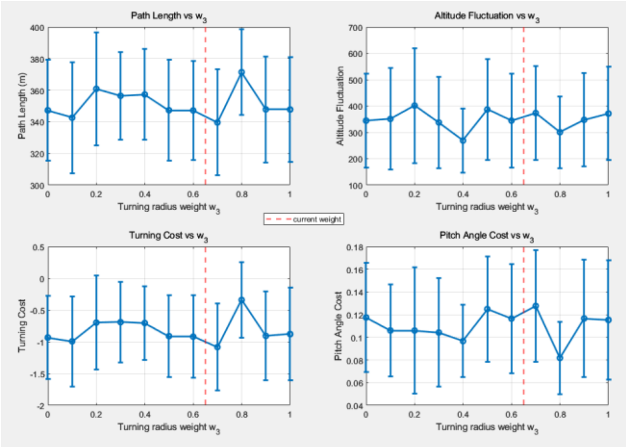

Fig. 7 - The influence of the turning radius weight w_3 on the performance of path planning

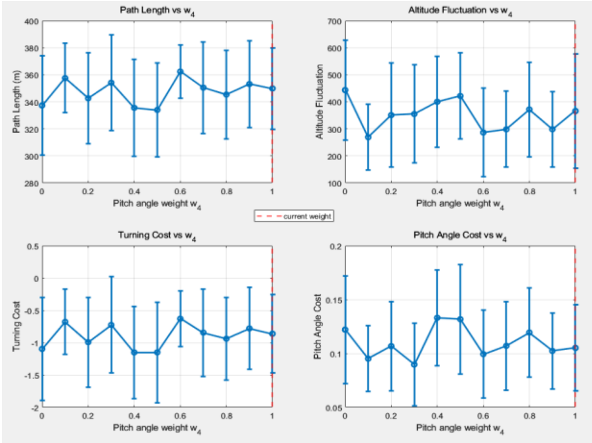

Fig. 8 - The influence of the pitch angle weight w_4 on the performance of path planning

Analysis Of Path Planning Simulation Results

To verify the robustness and effectiveness of the improved algorithms, this study conducted comparative experiments between the MDBO algorithm and several others, including PSO, COA, NGO, WOA, SSA, and DBO, in three mountainous environments with varying levels of complexity using MATLAB. The specific parameter settings for each algorithm are presented in Table 4.

Table 4

Parameter variable settings

Arithmetic	Algorithmic parameter	Numerical value
PSO	w	1
	c_1	1.5
	c_2	2.0
COA	w	Reduction from 1 to 0.1
	SF	1.5
NGO	w	Reduced linearly from 1 to 0.1
WOA	a	Decrease from 2 to 0
SSA	w	Reduced linearly from 1 to 0.1
	R	0.2
DBO	a	-1 or 1
	R	1(decreases linearly during iterations)
MDBO	R_1	$(0,2\pi)$
	R_2	$(0,\pi)$
	τ	$(\sqrt{5}-1)/2$
	a	-1 or 1
	R	1(decreases linearly during iterations)

To ensure the neutrality of the experimental outcomes, the parameters for all tested algorithms were uniformly configured. The starting point was set at coordinates (0, 0, 10), while the endpoint was at (200, 200, 30). The experiments maintained a population size of 50 and were capped at a maximum of 50 iterations.

The evaluation of path optimization performance across three different mountainous terrains of increasing complexity is depicted in Figures 9 and 10. Figure 9 provides a visual comparison of the pathfinding results of each algorithm, and Figure 10 explores the correlation between the number of iterations and the achievement of optimal values.

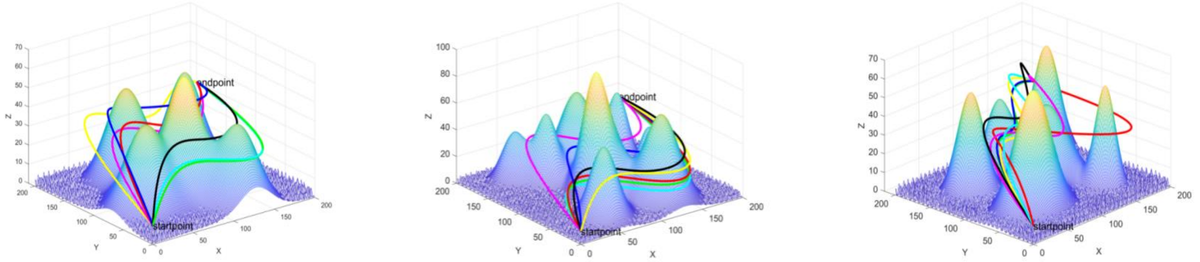

(a) Map 1 (b) Map 2 (c) Map 3

Fig. 9 - Comparison of air path planning effects

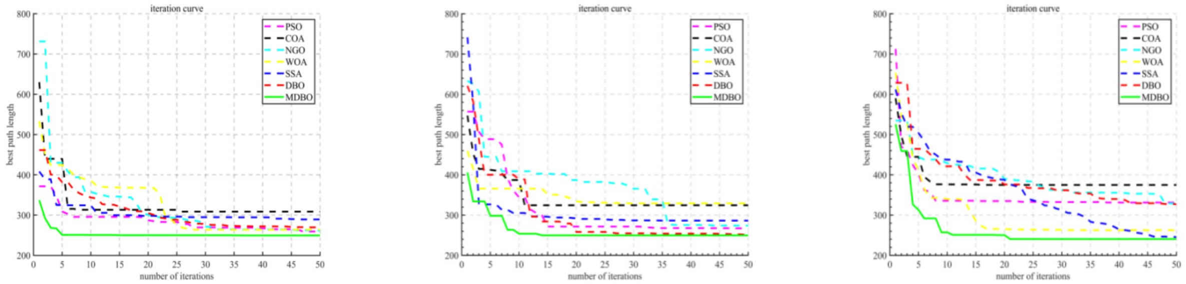

(a) Map 1 (b) Map 2 (c) Map 3

Fig. 10 - The iterations vs optimal value curve

The iteration curves of three maps are shown in Fig. 10. The improved MDBO achieves faster convergence and stronger early exploration capability than the basic DBO. All algorithms tend to converge before the 8th iteration, while MDBO consistently yields the best convergence value at each iteration, with both higher convergence speed and solution accuracy than other comparison algorithms. The golden sine strategy accelerates convergence, the dynamic adaptive weight prevents premature local trapping, and the adaptive Gaussian-Cauchy hybrid mutation further helps the algorithm escape from local optima. The phenomenon that the basic DBO is easily trapped in local optima during iteration also verifies the effectiveness of the above improvements.

To eliminate the influence of randomness, 30 independent runs are conducted for each map. As shown in Table 5, the proposed MDBO outperforms all other algorithms in terms of maximum, minimum and average path length. More importantly, MDBO achieves the minimum standard deviation, indicating higher stability and consistency in path planning performance.

Table 5

Individual evaluation indicators in different maps

Map	Algorithm	Longest path	Shortest path	Mean	Standard deviation
Map 1	PSO	340.42	272.02	299.21	19.08
	COA	366.97	263.53	298.23	30.52
	NGO	335.07	260.22	275.48	20.05
	WOA	364.10	251.00	301.20	34.24
	SSA	341.80	252.86	279.61	27.18
	DBO	326.14	246.52	267.60	21.02
	MDBO	**311.33**	**234.52**	**253.24**	**14.06**
Map 2	PSO	336.36	245.26	280.85	21.26
	COA	359.23	252.24	288.22	30.23
	NGO	319.55	247.83	275.73	20.52
	WOA	361.83	255.13	302.19	30.53
	SSA	324.33	243.64	265.02	20.10
	DBO	339.86	235.58	261.63	21.56
	MDBO	**301.84**	**220.90**	**245.17**	**16.98**
Map 3	PSO	339.05	255.56	292.94	18.39

Map	Algorithm	Longest path	Shortest path	Mean	Standard deviation
	COA	368.35	242.49	295.18	31.45
	NGO	326.61	238.14	279.57	23.70
	WOA	344.89	254.13	297.90	27.58
	SSA	333.16	238.35	269.99	29.11
	DBO	328.05	232.38	254.62	20.58
	MDBO	**296.99**	**226.94**	**239.47**	**14.26**

Ablation Experiment

The modified versions of the DBO algorithm are denoted in Table 6: DBO123 indicates the DBO algorithm equipped with the Bernoulli's chaotic mapping strategy, golden sine strategy and dynamic adaptive weighting strategy; DBO124 represents the DBO algorithm with the Bernoulli's chaotic mapping strategy, golden sine strategy and adaptive Gauss-Cauchy mixed-variance perturbation strategy; DBO234 means that the DBO algorithm uses golden sine strategy, dynamic adaptive weighting strategy and adaptive Gauss-Cauchy mixed-variance perturbation strategy.

Table 6

MDBO algorithm and its variants

Algorithm	Bernoulli's chaotic mapping	Golden sine	Dynamic adaptive weighting	Gauss-Cauchy mixed-variance perturbation
DBO123	√	√	√	
DBO124	√	√		√
DBO134	√		√	√
DBO234		√	√	√
MDBO	√	√	√	√

To confirm that simultaneously introducing the four strategies can improve the performance of the MDBO algorithm, a series of ablation experiments were designed. In three mountainous environments with different level of complexity, comparative experiments between MDBO with its variants DBO123, DBO124 and DBO234 were implemented using MATLAB. The parameter settings for all the experiments were the same, that is, the starting coordinate is (0,0,10), end coordinate is (200,200,30), population size 50 and maximum 50 iterations.

The path finding optimization of each algorithm across three mountain maps with varying levels of complexity is illustrated in Fig. 11 and Fig. 12. Fig. 11 presents a comparison of the path planning effectiveness, while Fig. 12 depicts the relationship between the number of iterations and the optimal values. A total of 30 experiments were conducted on each of the three maps, and the longest path, shortest path, average value, and standard deviation of the fixed-wing UAV in these experiments were statistically analyzed, as shown in Table 7.

Experimental results demonstrate that the complete MDBO algorithm outperforms all variant algorithms across all evaluation metrics, including maximum, minimum and mean path length, as well as standard deviation. Iteration curves further confirm that MDBO converges significantly faster on all test maps, and the synergy among multiple strategies substantially enhances its path planning capability in complex mountainous terrain.

These four complementary strategies empower MDBO to achieve superior 3D path planning for fixed-wing UAVs. Bernoulli mapping diversifies initial solutions, and the golden sine strategy accelerates convergence. Dynamic adaptive weights balance exploration and exploitation, while Gaussian-Cauchy hybrid mutation introduces stochastic perturbations to effectively escape local optima.

Table 7

Individual evaluation indicators in different maps

Map	Algorithm	Longest path	Shortest path	Mean	Standard deviation
Map 1	DBO123	323.27	240.17	259.09	23.60
	DBO124	322.76	243.04	260.92	19.78
	DBO134	314.13	243.16	259.15	18.86
	DBO234	322.06	243.14	257.30	17.64

Map	Algorithm	Longest path	Shortest path	Mean	Standard deviation
	MDBO	**298.55**	**230.32**	**250.38**	**12.77**
	DBO123	318.19	236.69	252.32	20.91
	DBO124	326.34	238.33	252.83	20.45
Map 2	DBO134	319.58	240.09	254.04	20.72
	DBO234	310.48	230.42	250.48	20.84
	MDBO	**295.11**	**220.50**	**246.09**	**16.32**
	DBO123	328.51	231.40	245.64	22.63
	DBO124	314.55	233.62	246.45	24.74
Map 3	DBO134	318.25	234.09	246.17	21.34
	DBO234	314.45	234.05	244.89	23.07
	MDBO	**296.71**	**220.89**	**238.68**	**16.26**

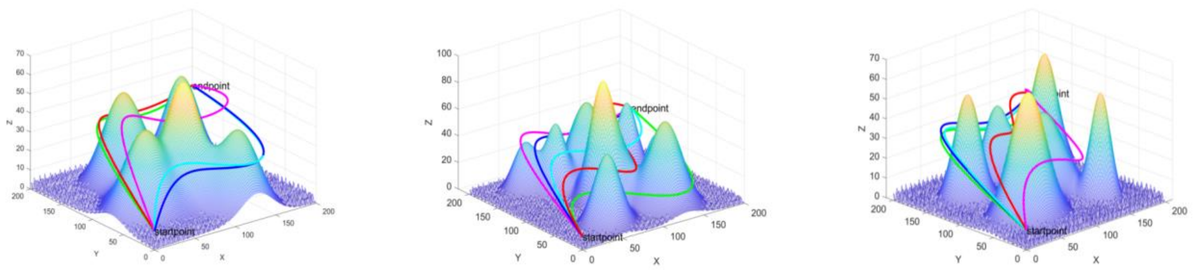

(a)Map 1 (b)Map 2 (c)Map 3

Fig. 11 - Comparison of air path planning effects

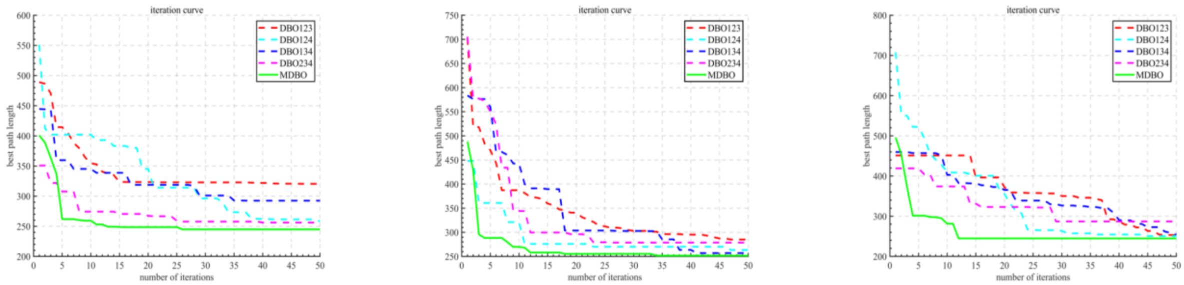

(a)Map 1 (b)Map 2 (c)Map 3

Fig. 12 - The iterations vs optimal value curve

Evaluation of Irrigation Effectiveness

Spray distribution quality of five algorithms (DBO123, DBO124, DBO134, DBO234 and MDBO) is evaluated on Map 1, with 30 independent runs conducted for each algorithm. Table 8 presents the statistical results of three irrigation indicators — coverage rate, overlap ratio and coverage uniformity, including the maximum, minimum, mean and standard deviation across all runs.

As shown in Table 8, MDBO achieves the highest coverage rate with the smallest standard deviation, indicating both optimal coverage performance and operational stability. The overall coverage rate of all algorithms is relatively low, mainly because fixed start and end points restrict path freedom, making a single flight unable to cover the entire map area; the safe turning radius and pitch angle constraints further narrow the feasible path space. Even under these limitations, MDBO still realizes relatively optimal coverage performance.

In addition, MDBO obtains the lowest overlap ratio, verifying its superior ability to avoid excessive spraying and minimize resource waste while maintaining adequate coverage. It also delivers the highest coverage uniformity, demonstrating its advantage in achieving balanced spray distribution. Comprehensive analysis confirms that the proposed MDBO algorithm achieves excellent overall irrigation performance.

Table 8

The irrigation index results of each algorithm in Map 1

Map	Performance indicators	Algorithm	Max	Min	Mean	Standard deviation
Map 1	Coverage rate	DBO123	0.1547	0.1121	0.1312	0.0089
		DBO124	0.1604	0.1158	0.1365	0.0100
		DBO134	0.1648	0.1294	0.1399	0.0114
		DBO234	0.1587	0.1163	0.1346	0.0099
		MDBO	**0.1734**	**0.1313**	**0.1449**	**0.0088**
	Overlap ratio	DBO123	0.1711	0.1087	0.1331	0.0133
		DBO124	0.1593	0.1258	0.1328	**0.0081**
		DBO134	0.1579	0.1262	0.1377	0.0117
		DBO234	0.1515	0.1203	0.1340	0.0083
		MDBO	**0.1474**	**0.1102**	**0.1267**	0.0091
	Uniformity	DBO123	0.6528	0.6054	0.6208	0.0139
		DBO124	0.6534	0.6046	0.6178	0.0151
		DBO134	0.6545	0.6057	0.6229	0.0175
		DBO234	0.6500	0.6058	0.6216	**0.0133**
		MDBO	**0.6617**	**0.6060**	**0.6362**	0.0167

CONCLUSIONS

This study addresses the core challenge of balancing obstacle avoidance safety and irrigation effectiveness in 3D path planning of fixed-wing UAVs for mountainous agricultural irrigation, and proposes a multi-strategy improved DBO (MDBO) algorithm with embedded flight kinematic constraints. Safe turning radius and pitch angle constraints are introduced to stabilize flight attitude and maintain irrigation consistency. Four improvement strategies (Bernoulli chaotic mapping, golden sine mechanism, dynamic adaptive weight, adaptive Gaussian-Cauchy hybrid mutation) are integrated to balance global exploration and local exploitation capability. Benchmark function tests and scenario simulation experiments verify the effectiveness of the proposed method.

Three irrigation performance indicators are established for posterior evaluation of spray distribution quality. Simulation results demonstrate that MDBO achieves superior performance in both path length optimization and irrigation effect, which fully meets the efficient irrigation path demands of mountainous crops.

This study is limited to simulation environment without considering practical factors such as wind disturbance, sensor noise and environmental variability, and irrigation indicators are applied for post-evaluation rather than being incorporated into the optimization objective. Future research will embed irrigation indicators into the objective function to balance path efficiency and irrigation quality, and further validate the algorithm via hardware-in-the-loop simulation and field tests.

ACKNOWLEDGEMENT

The authors were funded for this project by the Guizhou University Project (Guida Renjihezi (2023)52), (Guida Jichu [2023] 20), the Science and Technology Support Project of Guizhou Province, China (Qiankehe Support [2024] General 098), and the National Natural Science Foundation of China (Grant No.52465058), and the Guizhou Provincial Key Laboratory of Mountainous Intelligent Agricultural Machinery (Qiankehe Platform ZSYS[2025]013).

REFERENCES

[1] Chourasia S K, Vishwakarma S K, Pandey A. (2026). Can Micro-Irrigation in Canal Command Areas Increase Water Use Efficiency? A Feasibility Study for Sustainable Water Resources. *Water Conservation Science and Engineering*, Vol. 11, pp. 73, Roorkee/India.

[2] Hu R. P. (2023). Effectiveness of agricultural planting technology and agricultural mechanized production (农业种植技术与农业机械化生产的有效性). *Hebei Agricultural Machinery*, pp. 25-27, Hebei/China.

[3] Giagkiozis I, Purshouse R C, Fleming P J. (2015). An overview of population-based algorithms for multi-objective optimisation. *International Journal of Systems Science*, Vol. 46, pp. 1572-1599, Sheffield/United Kingdom.
[4] Wang S L, Song J L, He X K, et al. (2017). Performances evaluation of four typical unmanned aerial vehicles used for pesticide application in China. *Int J Agric & Biol Eng*, Vol. 10, pp. 22-31, Beijing/China.
[5] Wang C, Song J, He X, et al. (2017). Effect of flight parameters on distribution characteristics of pesticide spraying droplets deposition of plant-protection unmanned aerial vehicle (植保无人机飞行参数对施药雾滴沉积分布特性的影响). *Transactions of the Chinese Society of Agricultural Engineering*, Vol. 33, pp. 109-116, Beijing/China.
[6] Pan Z, Lie D, Qiang L, et al. (2016). Effects of citrus tree-shape and spraying height of small unmanned aerial vehicle on droplet distribution. *International Journal of Agricultural and Biological Engineering*, Vol. 9, pp. 45-52, Chongqing/China.
[7] Nanavati R V, Meng Y, Coombes M, et al. (2023). Generalized data-driven optimal path planning framework for uniform coverage missions using crop spraying UAVs. *Precision Agriculture*, Vol. 24, pp. 1497-1525, Loughborough/United Kingdom.
[8] Deng B C, Xu R, Huang C Y et al. (2022). Three-dimensional trajectory planning for unmanned aerial vehicles based on Kersey's variational sparrow search algorithm (基于柯西变异麻雀搜索算法的无人机三维航迹规划). *Mechanical Design and Research*, Vol. 38, pp. 62-66, Guangdong/China.
[9] Fadzli S A, Abdulkadir S I, Makhtar M, et al. (2015). Robotic indoor path planning using Dijkstra's algorithm with multi-layer dictionaries. *2015 2nd International Conference on Information Science and Security (ICISS)*, *IEEE*, pp. 1-4, Seoul/Korea.
[10] Zhou L, Li W. (2014). Adaptive artificial potential field approach for obstacle avoidance path planning. *2014 Seventh International Symposium on Computational Intelligence and Design*, *IEEE*, Vol. 2, pp. 429-432, Hangzhou/China.
[11] Zhu Q D, Yan Y J, Xing Z Y. (2006). Robot Path Planning Based on Artificial Potential Field Approach with Simulated Annealing. *Sixth international conference on intelligent systems design and applications*, Vol. 2, pp. 622-627, Jinan/China.
[12] Wang X, Liu Z, Liu J. (2023). Mobile robot path planning based on an improved A* algorithm. *International conference on computer graphics, artificial intelligence, and data processing (ICCAID 2022)*, Vol. 12604, pp. 1093, Guangzhou/China.
[13] Zhao Y, Li Y F. (2023). UAV pesticide spraying trajectory planning based on genetic algorithm (基于遗传算法的无人机农药喷洒航迹规划). *Intelligent Computer and Application*, Vol. 13, pp. 88-93+99, Shanghai/China.
[14] Wen J L, Liang F, Xu W. (2023). Research on three-dimensional path planning of unmanned aerial vehicle based on improved ant colony algorithm (基于改进蚁群算法的无人机三维路径规划研究). *Modern Information Technology*, Vol. 7, pp. 84-87+91, Zhejiang/China.
[15] Huang C. (2021). A Novel Three-Dimensional Path Planning Method for Fixed-Wing UAV Using Improved Particle Swarm Optimization Algorithm. *International Journal of Aerospace Engineering*, Vol. 1, pp. 7667173, Shenyang/China.
[16] Vazquez-Carmona E V, Vasquez-Gomez J I, Herrera-Lozada J C, et al. (2022). Coverage path planning for spraying drones. *Computers & Industrial Engineering*, Vol. 168, pp. 108125, Ciudad de México/México.
[17] Plessen M. (2025). Path planning for spot spraying with UAVs combining TSP and area coverages. *Smart Agricultural Technology*, Vol. 11, pp. 100965, Zug/Switzerland.
[18] Meron M, Peres M, Levin-Orlov V, et al. (2025). Irrigation uniformity assessment with high-resolution aerial sensors. *International Journal of Applied Earth Observation and Geoinformation*, Vol. 137, pp. 104446, Kiryat Shmona/Israel.
[19] Cui X, Han W, Zhang H, et al. (2023). Estimating soil salinity under sunflower cover in the Hetao Irrigation District based on unmanned aerial vehicle remote sensing. *Land Degradation & Development*, Vol. 34, pp. 84-97, Yangling/China.
[20] Xue J, Shen B. (2023). Dung beetle optimizer: a new meta-heuristic algorithm for global optimization: J. Xue, B. Shen. *The journal of Supercomputing*, Vol. 79, pp. 7305-7336, Shanghai/China.

[21] Jin H, Ji H, Yan F. (2023). An effective obstacle avoidance and motion planning design for underwater telescopic arm robots based on a tent chaotic dung beetle algorithm. *Electronics*, Vol. 12, pp. 4128, Huainan/China.
[22] Saito A, Yamaguchi A. (2016). Pseudorandom number generation using chaotic true orbits of the Bernoulli map. *Chaos: An Interdisciplinary Journal of Nonlinear Science*, Vol. 26, Hakodate/Japan.
[23] Du Y, Tian X Q, et al. (2024). Software defect detection method based on improved whale algorithm optimized SVM (基于改进鲸鱼算法优化 SVM 的软件缺陷检测方法). *Information Network Security*, Vol. 24, pp. 1152-1162, Beijing/China.